Thermal Decomposition Behavior of Poly[3,3-Bis(ethoxymethyl) Oxetane] and Related Polyethers

R. B. JONES, *Department of Chemistry, Materials Research Center No. 32, Lehigh University, Bethlehem, Pennsylvania 18015,* C. J. MURPHY,* *Materials Research Center No. 32, Lehigh University, Bethlehem, Pennsylvania 18015,* L. H. SPERLING, *Department of Chemical Engineering and Polymer Science and Engineering Program, Materials Research Center No. 32, Lehigh University, Bethlehem, Pennsylvania 18015,* M. FARBER and S. P. HARRIS, *Space Sciences, Inc., Monrovia, California 91016,* and G. E. MANSER, *Thiokol Wasatch Division, Brigham City, Utah 84302*

Synopsis

The thermal decomposition behavior of poly[3,3-bis(ethoxymethyl)oxetane] (polyBEMO) was examined and compared to the decomposition of poly(ethylene oxide) (PEO) and poly(tetramethylene oxide) (polyTHF). Differential scanning calorimetric (DSC) studies as a function of heating rates and at constant temperature as a function of time yielded activation energies of 45–50 kcal/mol, characteristic of polyether decomposition. First-order decomposition kinetics were found. The reaction is endothermic, with a heat of decomposition of 18.6 kcal/mol. Effusion mass spectroscopy on polyBEMO showed major peaks at 112, 140, 168, and 174 amu. A mechanism is proposed in which the thermal scission of the ether bonds in both the polymer chain and in the appendages initiates the decomposition. The main decomposition reaction for polyBEMO can be written as

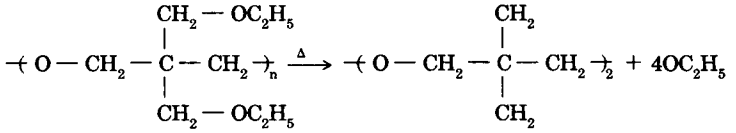

where the appendages and main chain are cleaved in an unknown order.

INTRODUCTION

The effect of elevated temperatures on the stability of polymers has received a great deal of attention due to high temperatures reached in processing[1] and also in certain high temperature applications such as the formulation of fire retardant polymers.[2-4] It is very important to know how to choose a polymer that will be thermally stable at temperatures of interest, although sometimes a knowledge of the conditions of instability are equally important.

* Permanent address: East Stroudsburg University, East Stroudsburg, PA 18301.

Journal of Applied Polymer Science, Vol. 30, 95–109 (1985)
 CCC 0021-8995/85/010095-15$04.00

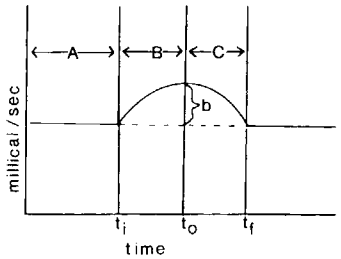

Fig. 1. Idealized DSC thermogram showing three regions of isothermal decomposition: (A) temperature-dependent induction period; (B) endothermic acceleratory period; (C) decay period.

Grassie[5,6] and Jamieson and McNeill[7] examined the decomposition behavior of poly(vinyl acetate) (PVA) and found that acetic acid was the major decomposition product. They suggest that the thermal degradation of PVA occurs by a free radical process involving the thermal scission of the C—O bond as the initiating step. This liberates an acetate radical, which abstracts a hydrogen atom from the polymer chain. The deacetylation from the adjacent monomer unit is then facilitated by allylic activation.

Madorsky and Straus[8] investigated the decomposition of poly(ethylene oxide) (PEO) and poly(propylene oxide) (PPO) finding that the main locus of bond cleavage was at the C—O bond. They attributed this to the greater C—C bond strength. Davis and Golden[9] found that the C—O bond was the primary bond broken in their work on poly(tetramethylene oxide) (poly-THF).* Blyumenfel'd and Kovarshaya[10] also studied the decomposition of polyTHF and found that indeed the ether bond was broken but suggested that its breakdown was caused by the scission of the C—C bond in the position α to the C—O bond.

In the present work, the decomposition kinetics of poly[3,3-bis(ethoxymethyl)oxetane] (polyBEMO), PEO, and polyTHF will be investigated by differential scanning calorimetry (DSC). Constant heating rate experiments will be used to find the enthalpy change upon decomposition, ΔH_D. Different heating rates will be employed to observe their effect on the decomposition temperature. Isothermal DSC techniques used by Beckmann et al.[11] and Rogers[12,13] will be applied to the polyethers. Analysis of the decomposition products will be accomplished by effusion mass spectroscopy following the method of Farber et al.[14]

THEORY

An idealized DSC isothermogram is shown in Figure 1. The curve can be divided into three regions[11]: (A) a temperature-dependent induction period, (B) an endothermic acceleratory period, and (C) the decay period. The baseline at the end of the decay period (C) can be extrapolated back to the original baseline. A vertical line drawn from the point of maximum heat absorption to the baseline defines the time t_0 indicating the start of the decomposition kinetic measurements. The height of the vertical line was designated b, and b was measured at regular time intervals from t_0 until the end of the decay period, t_f. According to Rogers,[12] b is directly proportional to the decomposition reaction rate, or

* Poly(tetramethylene oxide) is made from tetrahydrofuran (THF).

$$ab = \partial X/\partial t \tag{1}$$

where a is a proportionality constant and $\partial X/\partial t$ is the rate of decomposition.

Beckmann et al.[11] showed that the area under the decay portion of the endotherm is related to the extent of decomposition. A planimeter can be used to measure the total area (A_T) under the decay half of the endotherm. Fractional areas (A_P) are then measured at specific time intervals (P). The fraction decomposed (X) at any given time is given by

$$X = A_P/A_T \tag{2}$$

The fraction remaining at the end of each specific time interval (P) is then $1 - X$ and a rate expression for decomposition can be written as

$$\frac{\partial X}{\partial t} = k(1 - X)^n \tag{3}$$

where k is the rate constant for decomposition and n is the order of the reaction.

Equating eqs. (1) and (3) yields

$$b = k/a(1 - X)^n \tag{4}$$

Taking the natural logarithm of both sides of eq. (4) gives

$$\ln b = \ln(k/a) + n \ln(1 - X) \tag{5}$$

The order of decomposition can be determined from a plot of $\ln b$ vs. $\ln(1 - X)$.

For a first-order reaction, eq. (3) can be integrated to yield

$$\ln(1 - X) = -kt + c \tag{6}$$

where c is an integration constant.

Substituting eq. (6) into eq. (5) gives

$$\ln b = \ln(k/a) - kt + c \tag{7}$$

or

$$\ln b = -kt + D \tag{8}$$

where D is a constant equal to $\ln(k/a) + c$. Therefore, a plot of $\ln b$ vs. t should be linear with a slope of $-k$.

An alternate expression for the rate of decomposition can be developed that takes into account the entire area under the endotherm, and not just the portion in region C. For a first order reaction, eq. (2) can be substituted into eq. (3) and upon integration yields eq. (6) directly. From this a plot of $\ln(1 - X)$ vs. t should be linear with a slope of $-k$. Here again X is given

by eq. (2). However, A_T in this case is the total area under the endotherm and A_P is the area at specific time intervals P taken from the time at the beginning of the endotherm, t_i, to the time corresponding to the restoration of the baseline, t_f.

Region A of the decomposition thermogram constitutes the induction period which is characterized by the generation of catalytic substances. Catalysts can either be free radicals, anions, cations, or small molecules such as HCl which catalyze the decomposition of PVC.[15,16] When present in sufficient amounts, these catalysts initiate the decomposition. The induction period is of duration t_I, which is temperature-dependent. When ln t_I is plotted vs. $1/T$, an activation energy is obtained for the induction period.[11]

EXPERIMENTAL

Materials

Burdick and Jackson UV grade THF and methylene chloride were dried and stored over molecular sieves. Commercial grade boron trifluoride etherate was freshly distilled in vacuo before use. 1,4-Butanediol was distilled from calcium hydride and stored over molecular sieves. 3,3'-Bis(ethoxymethyl) oxetane (BEMO) monomer was prepared by the reaction of sodium ethoxide with bis(chloromethyl) oxetane in refluxing ethanol. BEMO monomer was freshly distilled from calcium hydride before use. All glassware was flame-dried and swept with dry nitrogen immediately preceeding the introduction of the reactants. During polymerization, the reactants were maintained under a dry nitrogen atmosphere.

The synthesis of polyBEMO goes as follows. A flame dried resin flask was charged with 1.296 g (0.0144 mol) of 1,4-butanediol dissolved in 50 mL of methylene chloride. The solution was cooled to 0°C and then 4.075 g (0.0287 mol) of boron trifluoride etherate was added dropwise. After this solution was stirred for a further hour, a solution containing 100 g (0.5747 mol) of BEMO in 450 mL of methylene chloride was added over a 20-min period. The reactor temperature was maintained at 0°C for the 36-h polymerization time. The solution was then quenched with 10 mL of saturated aqueous sodium chloride, and the organic phase washed with an equal volume of 10% aqueous sodium bicarbonate. The resultant polymer was isolated by precipitation from a tenfold volume excess of methanol and dried to constant weight under high vacuum at ambient temperature.

PEO was used as received from Aldrich Chemical Co. The PEO obtained was a white powder and had an average molecular weight of 100,000 g/mol.

PolyTHF was obtained from Quaker Oats, Inc. The material received was purified by dissolving it in twice its volume of methylene chloride and then reprecipitating from a fivefold volume excess of cold methanol. The precipitate was then dried to constant weight under vacuum at ambient temperature.

Instrumental

All DSC measurements were made on a Perkin-Elmer DSC 1-B. Calibration was made in the decomposition range using tin (T_m = 505 K) and lead

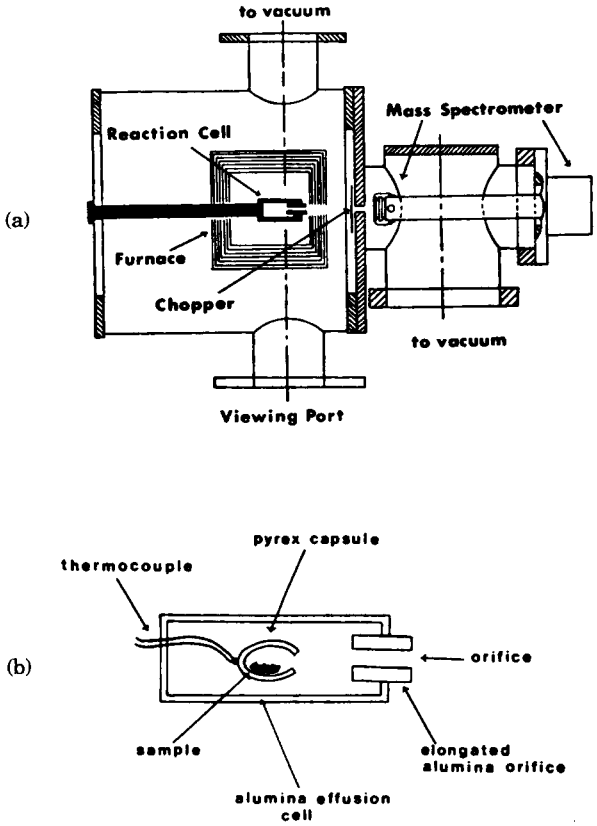

Fig. 2. Effusion mass spectroscopy: (a) dual vacuum mass spectrometer used to analyze decomposition products; (b) sample cell within effusion cell with elongated orifice.

(T_m = 600 K) standards obtained from Perkin-Elmer. In all cases the sample sizes were 5–10 mg. The samples were placed in aluminum pans, weighed, and crimped. The sample pan was then placed in one sample holder while a Perkin-Elmer reference pan was placed in the other.

Samples were decomposed by programming the DSC to one of eight heating rate positions and recording the heat change as a function of temperature through decomposition. The heating rates employed were 0.625, 1.25, 2.5, 5, 10, 20, 40, and 80°C/min. This produced thermograms which were plots of mcal/s vs. temperature.

Isothermal decomposition studies were patterned after techniques for low molecular weight organic and inorganic molecules.[11–13,17,18] The DSC was programmed to the temperature of interest and allowed to equilibrate for approximately five minutes. The sample was then placed in the sample holder and the recorder turned on. The resulting thermograms were a plot of mcal/s vs. time at a constant temperature.

Analysis of the decomposition products was accomplished by effusion mass spectroscopy. Details of the dual vacuum chamber-quadrupole mass spectrometer system used in these experiments have been presented previously.[14,19] A schematic of the apparatus is shown in Figure 2(a). The polymer samples, 5–50 mg in size, were placed in a small Pyrex capsule within an alumina effusion cell 25 mm long, with an inside diameter of 6.8 mm;

an elongated orifice 0.75 mm in diameter by 5.5 mm long was employed for beam collimation. Details of the effusion cell can be seen in Figure 2(b). The cell was positioned within 5 cm of the ionization chamber of the mass spectrometer allowing species leaving the solid or liquid surface to be measured within 10 μs after their exit from the cell. The alumina cell was heated by a resistance furnace, and temperature measurements were made by thermocouples imbedded in the cell body. The method of determining ion intensities, mass spectrometer resolution, as well as the measurement of the isotopic abundance ratios, has been presented previously.[20] All quadrupole experimental mass discrimination effects were taken into account and the necessary corrections to ion intensity relationships were made. Only the chopped, or shutterable, portion of the intensities were recorded, since the mass spectrometer was equipped with a beam modulator and a phase sensitive amplifier. The experimental procedure has been described previously in detail.[14,20-24] ^{127}I and $^{254}I_2$ as well as the standard gases N_2, O_2, NO_2, NO, H_2, and NH_3 were employed for the atomic mass unit (amu) calibration. Partial pressures were obtained from the calibrated data by means of

$$P_i = \frac{I_i(\sigma\gamma)_a}{I_a(\sigma\gamma)_i} \text{ Pa} \tag{9}$$

where a is the calibrated species, i is the unknown species, and σ and γ are, respectively, ionization cross sections and electron multiplier corrections.

It was necessary to ascertain with a high degree of confidence that the measured ion intensities were those from the parent species and not from the fragments of the larger molecules. In order to ensure the formation of ions from the parent species, the mass spectrometer was operated at low ionization voltage (as near as possible to appearance potentials; i.e., 1–2 V above their appearance potentials).[14,20-26]

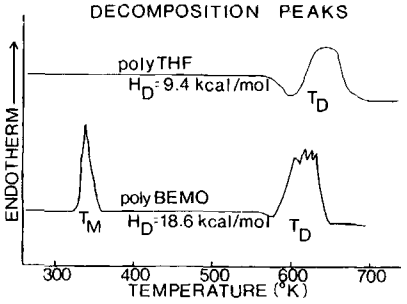

Fig. 3. Decomposition endotherms for polyBEMO and polyTHF obtained at a DSC heating rate of 10°C/min. By measuring the area underneath the endotherm ΔH_D, the enthalpy change upon decomposition is obtained.

TABLE I
DSC Decomposition Data of Polyethers

Polymer	ΔH_D (kcal/mol)	Decomposition range (°C)	Arrhenius-derived activation energy (kcal/mol)
PolyBEMO	18.6	270–355	47 ± 5
PolyTHF	9.4	322–382	50 ± 5
PEO	24.3	343–411	45.4 ± 5

RESULTS

PolyBEMO is a white powder with a melting temperature of 78°C and a glass transition of −35°C as measured by DSC. The molecular weight of polyBEMO was in the range of 15–25,000 g/mol. The physical properties of polyBEMO, together with its random and block copolymers, will be reported separately.[27]

Figure 3 shows the DSC decomposition peaks of polyBEMO and polyTHF at a heating rate of 10°C/min. Both peaks are broad and endothermic. PolyTHF exhibits a single peak whereas the polyBEMO decomposition has a number of fingerlike peaks through the endotherm. The enthalpy of decomposition ΔH_D can be calculated from the area underneath the decomposition curve. The values are given in Table I.

The decomposition temperature increases for each polymer as the heating rate is increased from 0.625°C/min to 80°C/min. The decomposition ranges are also given in Table I. A plot of the natural logarithm of the DSC heating rate vs. the reciprocal of the decomposition temperature can be seen in Figure 4 for polyBEMO and polyTHF. In both cases (also for PEO not shown), the plots were linear, and, from the slopes, activation energies were calculated and are shown in Table I. For the three polymers, activation energies in the range of 45–50 kcal/mol were obtained, apparently within experimental error of each other.

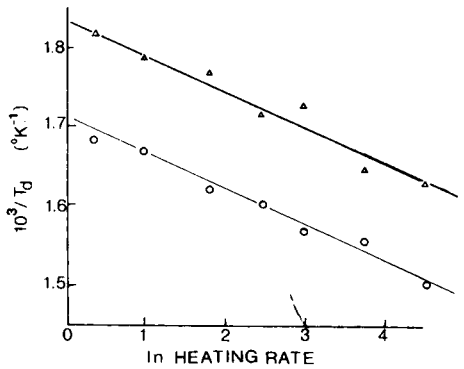

Fig. 4. Arrhenius-derived plots of $1/T_D$ vs. ln heating rate for polyBEMO (△) and polyTHF (○). From the slopes of these plots, the activation energy E_a [(△) 47 kcal/mol; (○) 50 kcal/mol] for the decomposition reaction was obtained.

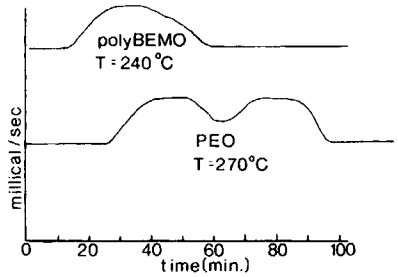

Fig. 5. DSC isothermograms for polyBEMO at 240°C and for PEO at 270°C.

Isothermal Decomposition

Figure 5 shows the isothermal decomposition peaks for polyBEMO at 240°C and for PEO at 270°C. The PEO curve is somewhat broader than the polyBEMO endotherm and shows a multipeak effect.

The order of the decomposition reaction can be obtained from a plot of $\ln b$ vs. $\ln(1\text{-}X)$ [eq. (6)]. Figure 6 shows such a plot for polyBEMO at 240°C. From the slope, the decomposition was found to be first order with respect to polyBEMO. Similar analysis for PEO proved difficult due to the multipeak effect. Taking the middle of the entire endotherm as the starting point yielded an order of 0.77 ± 0.21, which could either be first order or half order with respect to PEO. By taking the last peak as the starting point, an order of 0.91 ± 0.06 was obtained which is essentially first order with respect to PEO.

Figure 7 shows a plot of $\ln(1\text{-}X)$ vs. time which was used to calculate the rate constant k_D for the decomposition reaction:

$$\text{polymer} \xrightarrow{K_D} \text{decomposition products} \tag{10}$$

at a specific temperature. From the slope of this plot, a rate constant of $3.2 \times 10^{-3}\ s^{-1}$ at 240°C was obtained for polyBEMO. Similar analysis for PEO yielded a rate constant of $1.17 \times 10^{-2}\ s^{-1}$ at 270°C. Repeating this procedure at several temperatures and subsequent Arrhenius plots yielded activation energies of 49.7 and 47.1 kcal/mol for polyBEMO and PEO, respectively, ±5 kcal/mol.

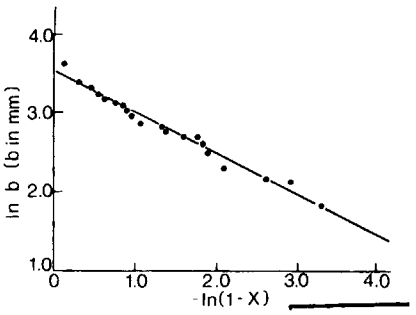

Fig. 6. Determination of the order of the decomposition reaction (polyBEMO). The order is the slope of a plot of ln b vs. $\ln(1\text{-}X)$: $T = 240$°C; $n = 0.98 \pm 0.05$.

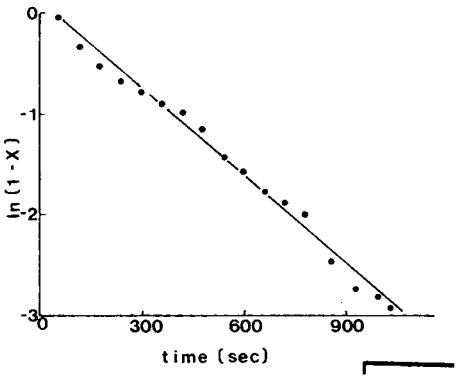

Fig. 7. Determination of the rate constant for decomposition. The rate constant is the slope of a plot of ln(1-X) vs. time at constant temperature. PolyBEMO: $T = 240°C$; $k_D = 3.2 \times 10^{-3}$ s^{-1}.

Table II summarizes the results from the isothermal DSC thermograms. Included in this table are the activation energies obtained from the Beckmann method,[11] which utilizes peak heights as a function of time to determine rate constants. Table II also shows activation energies for the induction period determined from plots of ln t_I vs. time for polyBEMO and PEO.

Effusion Mass Spectra

Mass spectral results were obtained at 100°C, 150°C, and 200°C (not shown). At 100°C polyBEMO seems to be thermally stable since no decomposition products were detected. At 150°C, there are three definite regions of decomposition products that occur, one at 45 amu, one at 70 amu, and one at 84 amu. At 200°C, decomposition is slightly more pronounced but appears in the same spectral region.

Figure 8 shows a composite mass spectrum of the decomposition products of polyBEMO at 230°C. The mass peaks at 15, 28, 29, 43, 112, 126, 140, and 168 amu are the most prominent. Peaks within the discreet mass ranges of 14–18, 26–31, 40–45, 56–84, and 112–212 amu are illustrated, for clarity.

Activation energies can be obtained from the mass spectral results via a van't Hoff plot, which is a plot of the natural logarithm of the relative peak intensity vs. the reciprocal of the temperature.

TABLE II
Isothermal Experiments on Polyethers

Polymer	Temperature range (°C)	Order	E_a[a]	E_a[b] (kcal/mol)	E_a[c]
polyBEMO	225–250	1st	52.4	49.7	17.8
PEO	255–280	1st	54.9	47.1	14.7

[a] Using peak heights as a function of time to determine rate constants (Beckmann et al.[11]).
[b] Using total area under the endotherm to determine rate constants (this study).
[c] Activation energy for induction period.

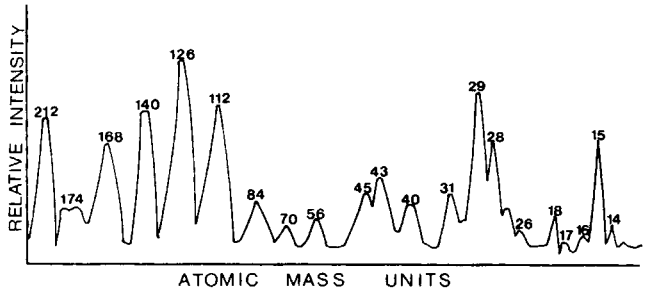

Fig. 8. Effusion mass spectrum showing the decomposition products of polyBEMO at 230°C.

Energy of activation values depend on the method of bond scission. The 98 amu peak, corresponding to C—C bond breaking, yielded an E_a value of 60 $\pm$ 10 kcal/mol in the temperature range of 220–230°C. On the other hand, the 112 amu peak, presumably corresponding to C—O bond rupture, yielded a slightly lower E_a value of 55 $\pm$ 10 kcal/mol.

A mass spectrum was also run on polyTHF. The major peak was at 72 amu, corresponding to the monomer tetrahydrofuran. Further work on polyTHF is in progress, and will be reported on separately.

DISCUSSION

It must be pointed out that the mechanism of thermal degradation of polymers depends strongly upon the experimental conditions. In this study, two quite different experiments were performed: DSC and EMS. In the DSC study, the sample was kept in a crimped pan, with the vaporous products escaping continuously. (At the end of the experiment, the pan is empty.) Moreover, air is present throughout the experiment. In the EMS experi-

TABLE III
Decomposition Ranges and Energies of Activation for Several Polyethers[a]

Polymer	Method of decomposition	Decomposition range (°C)	Energy of activation (kcal/mol)	Reference
PolyBEMO	DSC	270–355	47.0	Table I
	DSC	225–250	52.4	Table II
	DSC	225–250	49.7	Table II
	EMS	220–230	60.0	Results section
PEO	DSC	343–411	45.4	Table I
	DSC	255–280	54.9	Table II
	DSC	255–280	47.1	Table II
	Pyrolysis	324–363	46.0	8
PolyTHF	DSC	322–382	50.0	Table I
	TGA	265–340	49.4	9
	TGA	320–430	50.2	10
Poly(oxybutylethylene)	TGA	320–430	50.0	10
Isotactic PPO	Pyrolysis	285–300	45.0	8

[a] DSC = differential scanning calorimetry, TGA = thermogravimetric analysis, and EMS = effusion mass spectroscopy

ment, however, the degradation products are continuously carried away from the sample under vacuum conditions. In the following discussion, the differences between the experiments must be borne in mind, and correlations made rather cautiously.

Analysis of Kinetic Measurements

Table III shows a summary of experimental and literature results for several polyethers. In the case of polyTHF, the decomposition range of this study is in the middle of the ranges found by Davis and Golden[9] and Blyumenfel'd and Kovarshaya.[10] For PEO, the decomposition range of 343–411°C agrees with the findings of Madorsky and Straus.[8] PolyBEMO, of course, is the new polymer of interest.

The Arrhenius-derived activation energy for polyBEMO agrees well with activation energies obtained from isothermal experiments. The Arrhenius-derived value of 50 kcal/mol is identical within experimental error to the values of 49.4[9] and 50.2[10] kcal/mol for polyTHF. In the case of PEO, the value of 45.4 kcal/mol agrees well with the 46.0 kcal/mol found by Madorsky and Straus.[8]

The activation energy calculated by the Beckmann method, which plots ln b vs. time to determine rate constants, agrees within experimental error with the value found by the present method, which uses plots of $\ln(1 - X)$ vs. time to determine rate constants, for polyBEMO. However, there is a discrepancy in the case of PEO. The energy of activation found by the

TABLE IV

amu	Proposed structures
15	CH_3
29	C_2H_5
45	OC_2H_5
112	$-\!\!\left(O-CH_2-\underset{\displaystyle CH_2}{\overset{\displaystyle CH_2}{\overset{\displaystyle |}{\underset{\displaystyle |}{C}}}}-CH_2\right)\!\!-_2$
140	$-\!\!\left(O-CH_2-\underset{\displaystyle CH_2}{\overset{\displaystyle CH_2}{\overset{\displaystyle |}{\underset{\displaystyle |}{C}}}}-CH_2\right)\!\!-_2$
168	$-\!\!\left(O-CH_2-\underset{\displaystyle CH_2}{\overset{\displaystyle CH_2}{\overset{\displaystyle |}{\underset{\displaystyle |}{C}}}}-CH_2\right)\!\!-_2$
174	$-O-CH_2-\underset{\displaystyle CH_2OEt}{\overset{\displaystyle CH_2OEt}{\overset{\displaystyle |}{\underset{\displaystyle |}{C}}}}-CH_2-$

Beckmann method is 20% higher than the 46 kcal/mol found by Madorsky and Straus,[8] while the 47.1 kcal/mol found by the present method is nearly identical to their value.[8] The reason for the discrepancy lies in the multipeak endotherm (Fig. 5) exhibited by PEO. This type of endotherm is caused by complex decomposition reactions that take place and may occur in other polymeric decompositions. Treatment by the Beckmann method[11] is difficult because there is no set starting point for kinetic measurements. By using areas as a function of time to determine rate constants, the starting point is fixed at the beginning of the endotherm.

The energies of activation in Table III fall in the range 45–50 kcal/mol. This is somewhat lower than for the hydrocarbon analogs of these polyethers. For example, Jellinek[28] found an activation energy of 66.2 kcal/mol and Madorsky[29–31] found an activation energy of 72.06 kcal/mol for polyethylene, which is 20–26 kcal/mol higher than PEO. Also, Madorsky and Straus[29] found an activation energy of 58 kcal/mol while Davis et al.[32]

TABLE V
Possible Decomposition Routes for PolyBEMO

A. Main Chain Decomposition

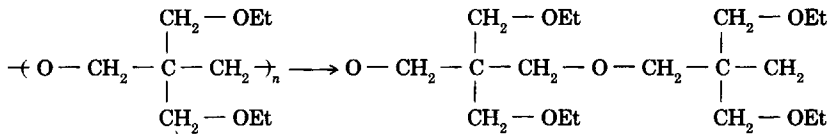

348 amu

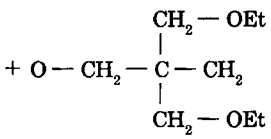

174 amu

B. Side Chain Decomposition

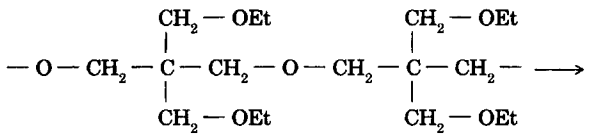

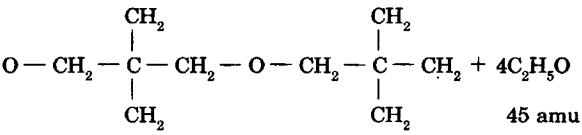

45 amu

168 amu

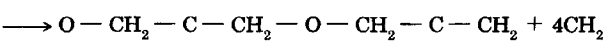

14 amu

126 amu

obtained 65.1 kcal/mol as an activation energy for isotactic polypropylene, which is 13–20 kcal/mol higher than isotactic poly(propylene oxide).

The value of 60 kcal/mol obtained by EMS at 98 amu is higher than the values reported through DSC, and the structure suggests C—C bond rupture. The value of 112 amu associated with the E_a value of 55 kcal/mol seems to support a C—O bond breakage (see Table IV).

Analysis of Mass Spectral Results

A composite mass spectra of the intensities of the mass peaks shown in Figure 8 are directly proportional only to the amount of each decomposition product within discreet mass ranges, i.e., 14–18, 26–31, 40–45, 56–84, and 112–212 amu. Table IV shows the major decomposition products and their proposed structures for polyBEMO.

Decomposition Mechanism

The possible routes to bond breakage and subsequent decomposition are shown in Table V. A mechanism for the decomposition of polyBEMO is proposed, bearing in mind the experimental limitations: The C—O bonds in the polymer chain break leaving only monomer and dimer units. The ether bonds in the appendages break more or less simultaneously leaving fragments at 112, 126, 140, and 168 amu (dimer) and 56, 70, and 84 amu (monomer). Although there is no dimer mass peak present (348 amu), the dimer apparently loses its ethoxy groups as follows:

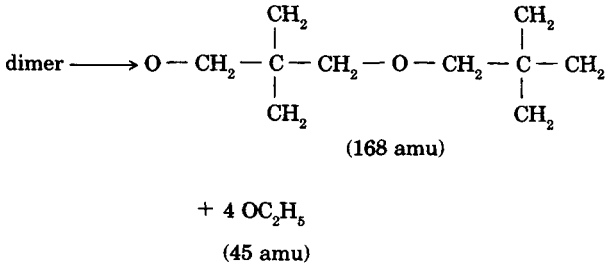

(11)

(168 amu)

$+ 4\ OC_2H_5$

(45 amu)

The 168 amu fragment then loses two, three, and then four methylene groups corresponding to mass peaks at 140, 126, and 112 amu and a mass peak at 14 amu for the methylene group. This is C—C bond breakage.

The same scenario is followed for the monomer unit except there is a peak at 174 amu corresponding to the monomer unit. The 174 amu species is stripped of its ethoxy groups in the following reaction:

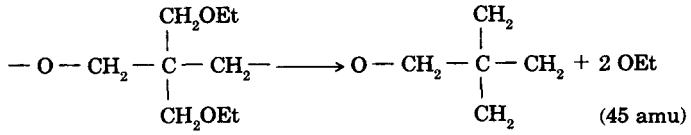

(12)

(45 amu)

(84 amu)

The methylene groups are then shed in a side reaction leaving mass peaks at 70 amu and 56 amu corresponding to the loss of 1 and 2 methylene groups, respectively.

The question of which C—O bond breaks first cannot be determined definitely from this study. Mass spectral results run at a series of temperatures show that initial decomposition occurs at 150°C. The spectrum at 150°C shows two species, one at 84 amu and another at 45 amu. The 84 amu species is the result of both C—O bonds C and D breaking leaving the monomer unit without the ethoxy groups (45 amu).

As noted in Figure 8, small quantities of masses 13, 14, 15, 16, 17, and 18 amu are also detected, corresponding to assorted small fragments. Thus, the evidence suggests that while both C—O and C—C bonds break in the side chains, the principal mode of backbone degradation is through C—O bond breakage to a mixture of dimer and monomer.

CONCLUSIONS

PolyBEMO, PEO, and polyTHF all exhibit broad endothermic decomposition peaks at temperatures which were found to depend on the DSC heating rates. Plots of $1/T_D$ vs. ln heating rate yielded activation energies for decomposition of 45–50 kcal/mol for these polyethers. Such plots provide a rapid method of determining activation energies of decomposition for these polyethers.

A method was developed for the treatment of isothermal DSC data in which the whole area under the endotherm is used to obtain kinetic parameters. This method was found to be in agreement with the previous method.[11] The current method provides a set starting point for kinetic measurements in the case of multipeak endotherms which occur due to complex decomposition processes. This method should be especially good for polymeric decompositions. First-order decomposition kinetics were found for polyBEMO.

A scheme was developed wherein the principle decomposition reaction could be written:

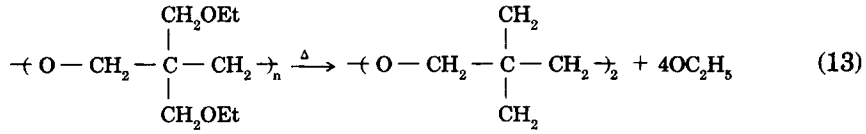

(13)

where the appendages and the main chain are cleaved in an unknown order.

The authors wish to thank the Office of Naval Research for support under contract No. N00014-82-K-0050 Mod. P00001.

References

1. S. Wolkenbreit, in *Handbook of Thermoplastic Elastomers*, Van Nostrand Reinhold, New York, 1979, Chap. 5.
2. G. Camino and L. Costa, *Polym. Deg. Stab.*, **3**, 423 (1981).
3. G. Camino, L. Costa, and L. Trossarelli, *Polym. Deg. Stab.*, **4**, 133 (1982).
4. L. Costa, G. Camino, and L. Trossarelli, *Polym. Deg. Stab.*, **5**, 267 (1983).
5. N. Grassie, *Trans. Faraday Soc.*, **48**, 379 (1952).
6. N. Grassie, *Trans. Faraday Soc.*, **49**, 835 (1953).
7. A. Jamieson and I. C. McNeill, *J. Polym. Sci., Polym. Chem. Ed.*, **14**, 1839 (1976).
8. S. L. Madorsky and S. Straus, *J. Polym. Sci.*, **36**, 183 (1959).
9. A. Davis and J. H. Golden, *Makromol. Chem.*, **81**, 38 (1965).

10. A. B. Blyumenfel'd and B. M. Kovarshaya, *Polym. Sci. USSR*, **12**, 710 (1970).
11. J. W. Beckmann, J. S. Wilkes, and R. R. McGuire, Thermochim. Acta, **19**, 111 (1977).
12. R. N. Rogers, *Anal. Chem.*, **44**, 1336 (1972).
13. R. N. Rogers and L. C. Smith, *Thermochim. Acta*, **1**, 1 (1970).
14. M. Farber, M. A. Fresch, and H. C. Ko, *Trans. Faraday Soc.*, **65**, 3202 (1969).
15. D. Braun and R. F. Bender, *Eur. Polym. J. Suppl.*, 229 (1969).
16. R. R. Stromberg, S. Straus, and B. G. Achhammer, *J. Polym. Sci.*, **35**, 355 (1959).
17. E. A. Dorko, R. S. Hughes, and C. R. Downs, *Anal. Chem.*, **42**, 253 (1970).
18. R. N. Rogers and E. D. Morris, *Anal. Chem.*, **38**, 412 (1966).
19. M. Farber and R. D. Srivastava, *Combust. Flame*, **42**, 165 (1981).
20. M. Farber and R. D. Srivastava, *Combust. Flame*, **20**, 33 (1973).
21. M. Farber, R. D. Srivastava, and O. M. Uy, *J. Chem. Soc., Faraday Trans. I*, **68**, 249 (1972).
22. M. Farber and R. D. Srivastava, *J. Chem. Soc., Faraday Trans. I*, **70**, 1581 (1974).
23. M. Farber and R. D. Srivastava, *J. Chem. Soc., Faraday Trans. I*, **73**, 1692 (1977).
24. M. Farber and R. D. Srivastava, *Chem. Phys. Lett.*, **51**, 307 (1977).
25. M. Farber, R. D. Srivastava, and J. M. Moyer, *J. Chem. Thermodyn.*, **14**, 1103 (1982).
26. M. Farber and R. D. Srivastava, *J. Chem. Phys.*, **74**, 2160 (1981).
27. K. E. Hardenstine, R. B. Jones, C. J. Murphy, G. E. Manser, and L. H. Sperling, *J. Appl. Polym. Sci.*, to appear.
28. H. H. G. Jellinek, *J. Polym. Sci.*, **4**, 13 (1949).
29. S. L. Madorsky and S. Straus, *J. Res. Natl. Bur. Stand.*, **53**, 361 (1954).
30. S. L. Madorsky, *J. Polym. Sci.*, **9**, 133 (1952).
31. S. L. Madorsky, *J. Res. Natl. Bur. Stand.*, **62**, 219 (1959).
32. T. E. Davis, R. L. Tobias, and E. B. Peterli, *J. Polym. Sci.*, **56**, 485 (1962).

Received February 15, 1984
Accepted May 10, 1984